Dynamics of Entanglement Networks of Rodlike Micelles Studied by Measurements of Ultrasonically Induced Birefringence

Keiji Yasuda,* Tatsuro Matsuoka, Shinobu Koda, and Hiroyasu Nomura

Department of Molecular Design and Engineering, Graduate School of Engineering, Nagoya University, Nagoya, 464-01, Japan

Received: October 8, 1996; In Final Form: December 2, 1996[⊗]

Ultrasonically induced birefringence was observed on the entanglement networks of the rodlike micelles of hexadecyldimethylammine oxide and mixtures of hexadecyltrimethylammonium bromide and sodium salicylate. After the onset of ultrasound, the birefringence increased suddenly and approached a steady value after a damped oscillation. The steady value of the birefringence was proportional to the ultrasonic intensity and increased with the ultrasonic frequency. The birefringence of the entanglement networks is induced by the radiation pressure. The period of oscillation and damping time constant of birefringence were related respectively to the plateau modulus and the stress relaxation time obtained from rheological measurement.

Introduction

Some surfactant molecules form rodlike micelles in aqueous solution.[1,2] In the dilute concentration range, the solutions of these surfactants behave like sols.[3] At higher concentrations, the rodlike micelles form entanglement networks and the solutions show pronounced viscoelasticity. The rodlike micelles are anisotropic aggregates and the solutions become birefringent by application of external fields. The dynamics of the entanglement networks of the rodlike micelles has been investigated by birefringence measurements such as electric birefringence[4] and flow birefringence.[5−7] The results of studies showed some anomalous behaviors characteristic of the entanglement networks.

Hoffmann *et al.*[4] investigated the rodlike micelles of hexadecyloctyldimethylammonium bromide by electric birefringence. They indicated that the four different relaxation processes appeared with changing the micelle concentrations. In the dilute range, a birefringence was observed with a first relaxation time which resulted from the orientation of the individual rods whose relaxation time was about 10^{-6} s. The length of rodlike micelles estimated from the first relaxation time agreed with that determined by light scattering.[1] The overlaping of the rodlike micelles gives rise to a second relaxation process, having a relaxation time of about 10 times longer than that of the first process. In the concentrated region where the rodlike micelles form the network, a third and fourth process appeared in the ranges from 1 to 10 ms and from 10 to 100 ms, respectively. For many rodlike micelles, the fourth relaxation time is close to the stress relaxation time determined by rheological measurements.[4,8] They considered that the second process comes from a coupled rotational translational motion and the third and the fourth processes are due to the orientational motion of rods and deformational motion of the entanglement networks. However the details of the second, third, and fourth relaxation processes have not been clarified yet,[8] and one of reasons is the difficulty in estimating the thickness of the electric double layer in rodlike micelles.

Shikata *et al.*[5] examined the mixtures of hexadecyltrimethylammonium bromide and sodium salicylate by transient flow birefringence and viscoelasticity. They clarified that for the entanglement networks of rodlike micelles the stress-optical law holds well under a shear rate less than 3 s^{-1}. However, under a shear rate greater than 3 s^{-1}, the time dependence of the orientation angle varied in a wavy fashion; this behavior was not completely reproducible and the stress-optical law no longer held. The wavy curve of flow birefringence was explained in terms of some drastic structural changes of the entanglement networks of micelles and also of the micelles themselves. However this interpretation is not proved by experiment. In flow birefringence, the shear rate is generally limited below 1000 s^{-1}. Information of birefringence under high shear rate or high frequency will help to elucidate the origin of the wavy curve of flow birefringence.

Double refraction is induced in liquids and solutions containing a certain amount of nonspherical particles when traversed by ultrasonic waves. This is called the phenomenon of ultrasonically induced double refraction.[9] Compared with other birefringence methods, the advantages of the ultrasonically induced birefringence method are that it enables us to investigate the motion of rodlike micelles under flow of high frequency and it is free from the presence of ions or an electric double layer rodlike micelle. The purpose of this work is to investigate the dynamics of the entanglement networks of rodlike micelles (hexadecyldimethylamine oxide) and rodlike micelles (mixtures of hexadecyltrimethylammonium bromide and sodium salicylate) by ultrasonically induced birefringence methods. The elastic property of the entanglement networks of the rodlike micelles will be discussed from the transient spectrum of ultrasonically induced birefringence.

Experimental Section

Samples. Hexadecyldimethylamine oxide (CDAO) was prepared according to the following method.[10,11] Hexadecyldimethylamine was purified by vacuum distillation and oxidized with H_2O_2 in ethanol. The products were dried by azeotropic distillation with toluene, ethanol, and benzene in order and were recrystallized twice from acetone. The recrystallized products were dried in vacuo at 65 °C for 8 h, and the purity of the products was checked by static light scattering measurement.[12] Hexadecyltrimethylammonium bromide (CTAB) and sodium salicylate (NaSal) were purchased from WAKO Pure Chemical Industries, LTD and were used without further purification. The concentrations of CDAO solutions were 10, 50, and 100 mM, while the concentration of CTAB was 30 mM

[⊗] Abstract published in *Advance ACS Abstracts,* January 15, 1997.

S1089-5647(96)03092-1 CCC: $14.00 © 1997 American Chemical Society

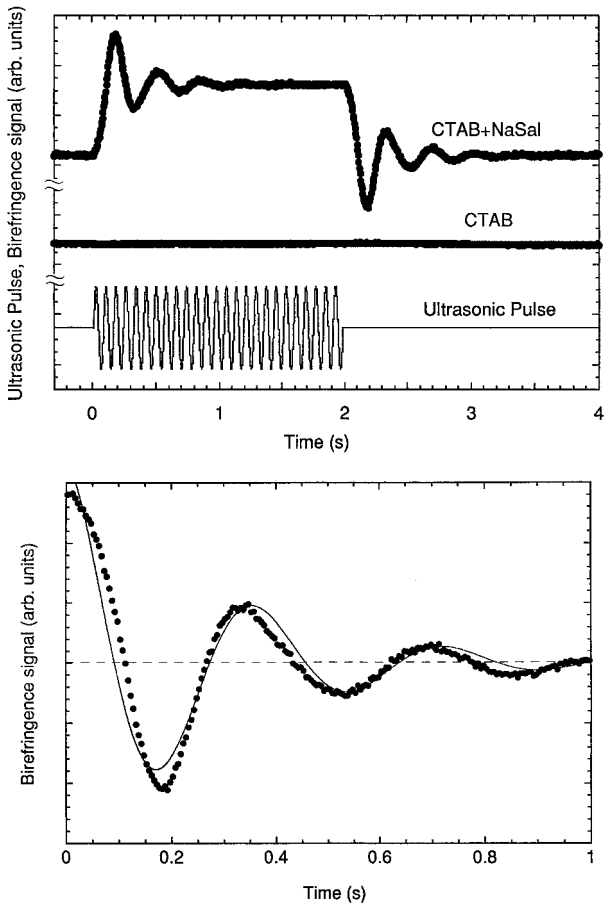

Figure 1. (a, top) Time dependence of the transient transmission light of the solution of 30 mM CTAB and mixtures of 30 mM CTAB and 230 mM NaSal at 35 °C (25 MHz, 0.058 W/cm^2) and the waveform of the pulse used. (b, bottom) Expanded illustration of the transient transmission light of mixtures of 30 mM CTAB and 230 mM NaSal after cessation of ultrasound. Solid curve refers to the calculated one given by $I(t) = \exp(-t/0.28)\cos(2\pi t/0.36)$.

and the concentrations of NaSal were 0 and 230 mM. Solutions were left standing for at least 7 days at 35 °C to reach equilibrium.

Birefringence Measurement. The difference of refractive index, $\Delta n = n_{\|} - n_{\perp}$, was measured in an ultrasonically induced birefringence experiment, where $n_{\|}$ and $n_{\perp}$ are refractive indexes parallel and perpendicular to the direction of sound wave propagation, respectively. The details of the ultrasonically induced birefringence apparatus have been well described elsewhere.[13−15] The ultrasonic intensities in the sample cell are determined by measuring the light intensities of the Bragg diffraction.[16]

In our measurements, the ultrasonic intensity was less than 0.06 W/cm^2 and the ultrasonic frequency was varied from 15 to 45 MHz. The pulse length was always long enough to reach the steady value of the ultrasonically induced birefringence, Δn_{st}. The aqueous solutions of CDAO display iridescence[17] at temperatures below 23 °C and become transparent and isotropic above 30 °C. The measurements were carried out at 35.0 ± 0.1 °C.

Results

Figure 1a shows the results of the ultrasonically induced birefringence measurement of solutions of 30 mM CTAB and mixtures of 30 mM CTAB and 230 mM NaSal together with the waveform of the ultrasonic pulse used. A birefringence signal was not observed for 30 mM CTAB. The CTAB forms spherical micelles above its critical micelle concentration (cmc = 0.92 mM).[18] When NaSal is added to CTAB solutions that lie above the cmc and the mole ratio NaSal/CTAB becomes greater than 0.3, rodlike micelles are formed. The mixtures of 30 mM CTAB and 230 mM NaSal form entanglement networks of rodlike micelles. Ultrasonically induced birefringence was observed for the entanglement networks. The birefringence after the onset of ultrasound increases suddenly and approaches a steady value after a damped oscillation. The waveform of transient birefringence of the CTAB−NaSal mixture after the cessation of ultrasound is consistent with the inverted waveform of transient birefringence after the onset of ultrasound. The sign of the induced birefringence is negative, and the value of Δn_{st} in Figure 1a is 7.4×10^{-9}. Figure 1b is an expanded illustration of birefringence of the mixtures of CTAB and NaSal after the cessation of ultrasound. The decay curve is expressed by a damped oscillation given as

$$\Delta n(t) = \Delta n_{st} \exp(-t/\tau_d) \cos(2\pi t/T) \qquad (1)$$

where τ_d is the damping time constant and T the period of oscillation. In Figure 1b, the solid curve is the fitted one using eq 1 with $\tau_d = 0.28$ s and $T = 0.36$ s and is in accordance with the experimental results.

Figure 2a gives the ultrasonically induced birefringence measurements observed for 10, 50, and 100 mM CDAO and the waveform of the ultrasonic pulse used. A birefringence signal is not observed for 10 mM CDAO. The CDAO begins to form rodlike micelles above its critical micelle concentration (cmc = 2.5×10^{-5} M),[19] and the entanglement networks of the rodlike micelles are formed above about 20 mM.[20] The ultrasonically induced birefringence was observed for the entanglement networks. For both concentrations, the sign of the induced birefringence was negative. The value of Δn_{st} of 100 mM was 2.5×10^{-9}, while for 50 mM it was 1.5×10^{-9}. Figure 2b indicates the time dependence of birefringence of 100 and 50 mM CDAO after the cessation of ultrasound. In Figure 2b, the solid curve is the calculated one using eq 1 with $\tau_d = 0.09$ s and $T = 0.10$ s for 100 mM and the dotted curve is the calculated value with $\tau_d = 0.13$ s and $T = 0.32$ s for 50 mM. These curves well reproduce the experimental results. The value of T increases with decreasing concentration, while the value of τ_d does not depend on the concentration of CDAO. It is interesting to note that the value of T of solutions of 50 mM CDAO is close to that of mixtures of 30 mM CDAO and 230 mM NaSal.

Figure 3 shows the birefringence of 50 and 100 mM CDAO as a function of the ultrasonic intensity. The birefringence is proportional to the ultrasonic intensity for both concentration. We also analyzed the ultrasonic intensity dependence of τ_d and T. The values of τ_d and T did not depend on the ultrasonic intensity.

Figure 4 refers to the frequency dependence of the birefringence of 100 mM CDAO normalized for ultrasonic intensity, $\Delta n_{st}/W$. The $\Delta n_{st}/W$ increases with frequency. The frequency dependence of τ_d and T was analyzed, and the values of τ_d and T did not depend on ultrasonic frequency.

Discussion

Ultrasonically induced birefringence was observed on the entanglement networks of rodlike micelles. The birefringence of the entanglement networks of the rodlike micelles was proportional to the ultrasonic intensity and increased with the ultrasonic frequency.

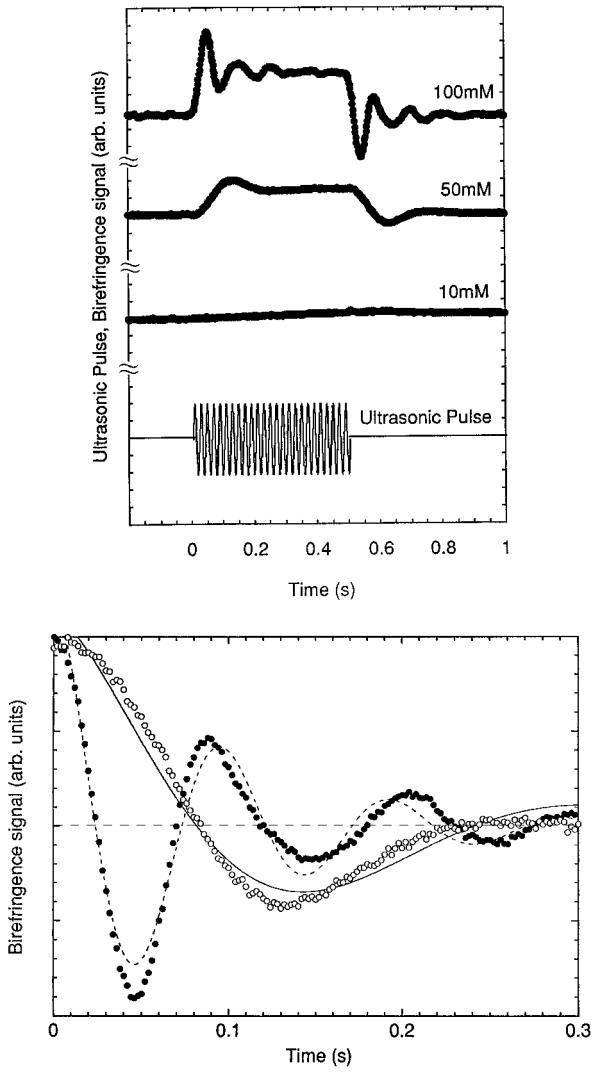

Figure 2. (a, top) Time dependence of the transient transmission light of 10, 50, and 100 mM CDAO at 35 °C (25 MHz, 0.058 W/cm^2) and the waveform of the pulse used. (b, bottom) Expanded illustration of the transient transmission light of CDAO after cessation of ultrasound: (●) 100 mM; (○) 50 mM. Dotted curve shows the calculated value with $I(t) = \exp(-t/0.09)\cos(2\pi t/0.10)$. Solid curve shows the calculated value with $I(t) = \exp(-t/0.13)\cos(2\pi t/0.32)$.

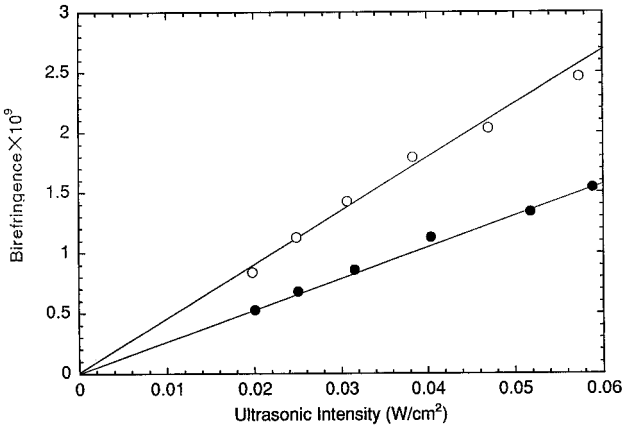

Figure 3. Birefringence of CDAO against ultrasonic intensity at 35 °C (25 MHz): (○) 100 mM; (○) 50 mM.

For solutions of flexible macromolecules, Peterlin[21,22] gave a theory of the ultrasonically induced birefringence. According to the theory, the birefringence comes from the deformation of flexible macromolecules due to the velocity gradient of the sound wave. Then the birefringence of flexible macromolecules

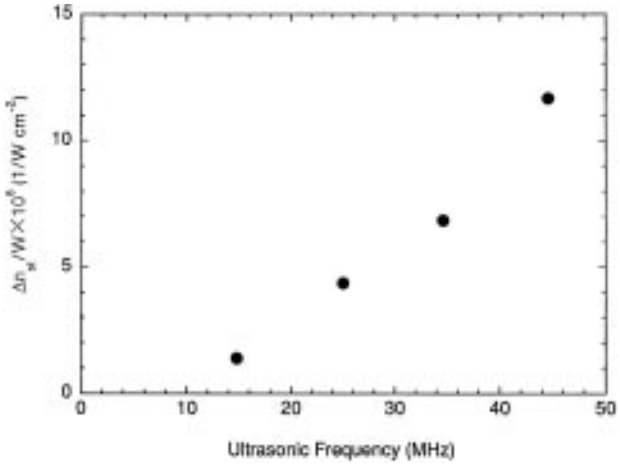

Figure 4. Frequency dependence of the birefringence for unit ultrasonic intensity at 100 mM CDAO.

is proportional to the square roots of ultrasonic intensity. As the birefringence of the rodlike micelles is proportional to the ultrasonic intensity, the birefringence is not interpreted in terms of the Peterlin theory. The birefringence for dilute solutions of rigid colloidal particles is formulated by Oka.[22,23] If the ultrasonic frequency is much higher than the rodlike particle reorientational frequency, the radiation pressure due to the propagation of the sound wave causes a turning torque which aligns the minor axis of the particle to the direction of the ultrasonic wave propagation.[13] Consequently, the birefringence of colloidal particles is proportional to the ultrasonic intensity. The ultrasonic intensity dependence of the birefringence of the entanglement networks indicates that the birefringence is induced by the radiation pressure. The frequency dependence of the birefringence results from the translational velocity difference between the entanglement networks and the solvent. With increasing ultrasonic frequency, the translational motion of entanglement networks with respect to solvent becomes harder. As the radiation pressure on the rodlike micelles increases with the translational velocity difference, the birefringence increases with the ultrasonic frequency.

No theory has been proposed yet that can explain the damped oscillation behavior of transient ultrasonically induced birefringence of the rodlike micelles. The viscoelastic properties[18,20,24] of the entanglement networks of CDAO and the mixtures composed of CTAB and NaSal have been described by a Maxwell model that has only one stress relaxation time, τ_s, and the entanglement networks are regarded as an elastic body with a plateau modulus, G_0, at frequencies much higher than $1/\tau_s$. The shear stress[25] on the entanglement networks of the mixtures of CTAB and NaSal exhibited the damped oscillation at the start of shear flow of high rate above 0.24 s^{-1}. We considered the ultrasonically induced birefringence of rodlike micelles as follows. The entanglement networks suffer stress due to the radiation pressure of the ultrasonic wave and shrink in the direction of sound propagation with damping elastic oscillation. In the shrunken entanglement network, the major axis of the rodlike micelles is elongated and orientated perpendicularly to the direction of the ultrasonic wave propagation. After the cessation of ultrasonic fields, the entanglement networks relax from a shrunken state with damping elastic oscillation. Since the fact that G_0 of the entanglement networks is approximately proportional to the square of the concentration of surfactant molecules is essentially equal to that observed in entangling polymer systems, for example, rubber,[18,26] the period of damped oscillation of birefringence, T, is inversely proportional to the square root of G_0. The value of τ_d is the deformational

TABLE 1: Values of Period T and Damping Time Constant τ_d of a Damped Oscillation Given in Figures 1b and 2b, the Plateau Modulus G_0, and the Stress Relaxation Time τ_s

	mixtures of 30 mM CTAB and 230 mM NaSal	50 mM CDAO	100 mM CDAO
T/s	0.36	0.32	0.10
τ_d/s	0.28	0.13	0.09
G_0/Pa	4.4[a]	3.2[b]	10[c]
τ_s/s	2.5[a]	0.3[b]	0.3[c]

[a] Obtained at 25 °C.[24] [b] Obtained at 60 mM.[26] [c] Reference 26.

relaxation time of the entanglement networks. Because τ_s comes from the movement of entanglement networks as a whole, the value of τ_d increases with τ_s. Table 1 indicates τ_s and G_0, as well as τ_d and T. The value of T decreases with increasing G_0. Since the G_0 of 60 mM CDAO is comparable to that of the mixtures of CTAB and NaSal, the value of T of 50 mM CDAO is close to that of the mixtures of CTAB and NaSal. For CDAO, values of both τ_s and τ_d are independent of concentration. The value of τ_d increases with the value of τ_s for CDAO and the mixtures of CTAB and NaSal. The quantitative relationships between G_0 and T and between τ_d and τ_s are not clear, since available data of τ_s and G_0 are few.

The sign of the birefringence depends on whether the orientational direction of the major axis of the rodlike micelles is perpendicular or parallel to the propagation of the sound wave and whether the birefringence is caused by the positive form birefringence of the rodlike micelles or the negative intrinsic birefringence of the surfactant monomers.[4] In the ultrasonically induced birefringence measurements, the signs of birefringence were negative. The negative birefringence can be explained in two different ways. In one way, the orientational direction of the major axis of the rodlike micelles with the positive form birefringence of the rodlike micelles is perpendicular to the propagation of the sound wave. In the other, the orientational direction of the major axis of the rodlike micelles with negative intrinsic birefringence of the surfactant monomers is parallel to the propagation of the sound wave. The results of flow birefringence measurements[5] show that the birefringence is caused by the negative intrinsic birefringence of the surfactant monomers. As described in the above section, the major axis of the rodlike micelles is elongated and orientated perpendicularly to the direction of ultrasonic wave propagation. The ultrasonically induced birefringence might be caused by the positive form birefringence of the rodlike micelles.

To study the rigidity of micelles and the salt dependences of damping oscillation of ultrasonically induced birefringence of rodlike micelles, we now are measuring the birefringence of rodlike micelles composed of mixtures of CTAB and NaSal.

Acknowledgment. We would like to express our sincere thanks to Prof. Imae, Nagoya University, for her valuable suggestions and Prof. Shikata, Osaka University for providing data of elasticity of CDAO. We wish to thank Mr. Takahashi and Mr. Tachibana, Work Shop for Experimentation and Practice, School of Engineering, Nagoya University, for constructing the acoustic cell. This work is partly supported by a Grant-in-Aid from the Ministry of Education, Science and Culture (No. 06640743).

References and Notes

(1) Hoffmann, H.; Oetter, G.; Schwandner, B. *Prog. Colloid Polym. Sci.* **1987**, *73*, 95.
(2) Pilsl, H.; Hoffmann, H.; Hofmann, S.; Kalus, J.; Kencono, A. W.; Lindner, P.; Ulbricht, W. *J. Phys. Chem.* **1993**, *97*, 2745.
(3) Rehage, H.; Hoffmann, H. *J. Phys. Chem.* **1988**, *92*, 4712.
(4) Hoffmann, H.; Krämer, U.; Thurn, H. *J. Phys. Chem.* **1990**, *94*, 2027.
(5) Shikata, T.; Dahman, S. J.; Pearson, D. S. *Langmuir* **1994**, *10*, 3470.
(6) Hofmann, S.; Rauscher, A.; Hoffmann, H. *Ber. Bunsen-Ges. Phys. Chem.* **1991**, *95*, 153.
(7) Hu, Y.; Wang, S. Q.; Jamieson, A. M. *J. Colloid Interface Sci.* **1993**, *156*, 31.
(8) Hoffmann, H.; Rauscher, A.; Gradzielski M.; Schulz S. F. *Langmuir* **1992**, *8*, 2140.
(9) Kawamura, H. *Kagaku (Tokyo)* **1938**, *7*, 6, 54, 139 (in Japanese).
(10) Abe, A.; Imae, T.; Shibuya, A.; Ikeda S. *J. Surf. Sci. Technol.* **1988**, *4*, 67.
(11) Devinsky, F.; Leitmanova, A.; Lacko I.; Krasnec L. *Tetrahedron* **1985**, *41*, 5707.
(12) Imae, T. *J. Jpn. Oil Chem. Soc.* **1992**, *41*, 616.
(13) Yasuda, K.; Matsuoka T.; Koda S.; Nomura, H. *J. Phys. Chem.* **1996**, *100*, 5892.
(14) Yasuda, K.; Matsuoka T.; Koda S.; Nomura, H. *Jpn. J. Appl. Phys.* **1994**, *33*, 2901.
(15) Koda, S.; Koyama, T.; Enomoto, Y.; Nomura, H. Proceedings of the 12th Symposium of Ultrasonic Electronics, Tokyo, 1991. *Jpn. J. Appl. Phys., Part 1* **1992**, *31*, Suppl. 31-1, 51.
(16) Bragg, W. H.; Bragg, W. L. *X-rays and Crystal Structure*; Bell: London, **1915**.
(17) Imae, T.; Sasaki, M.; Ikeda S. *J. Colloid Interface Sci.* **1989**, *131*, 601.
(18) Shikata, T.; Kotaka, T. *J. Non-Cryst. Solids* **1991**, *131*−*133*, 831.
(19) Platz, G.; Thunig, C.; Hoffmann, H. *Prog. Colloid Polym. Sci.* **1990**, *83*, 167.
(20) Hashimoto, K.; Imae, T. *Langumir* **1991**, *7*, 1734.
(21) Peterlin, A. *Recl. Trav. Chim. Pays-Bas* **1950**, *69*, 14.
(22) Hilyard, N. C.; Jerrard, H. G. *J. Appl. Phys.* **1962**, *33*, 3470.
(23) Oka, S. *Kolloid Z.* **1939**,87,37; *Z. Phys.* **1940**, *116*, 632 (in German).
(24) Wheeler, E. K.; Izu, P.; Fuller, G. G. *Rheol. Acta* **1996**, *35*, 139.
(25) Shikata, T.; Hirata, H.; Takatori, E.; Osaki, K. *Non-Newtonian Fluid Mech.* **1988**, *28*, 171.
(26) Shikata, T. Private communication.